ELSEVIER

Ultrasonics Sonochemistry 9 (2002) 133–138

Ultrasonics SONOCHEMISTRY

www.elsevier.com/locate/ultsonch

A dissolution and reaction modeling for hydrolysis of TEOS in heterogeneous TEOS–water–HCl mixtures under ultrasound stimulation

Dario A. Donatti, Alberto Ibañez Ruiz, Dimas R. Vollet *

Department of Physics, IGCE, UNESP, 13500-230 Rio Claro, SP, Brazil

Received 9 July 2001; accepted 24 September 2001

Abstract

A simplified dissolution and reaction modeling was employed to study the hydrolysis of heterogeneous tetraethoxysilane (TEOS)–water–HCl mixtures under ultrasound stimulation. The nominal pH was changed from 0.8 to 2.0. The acid specific hydrolysis rate constant was determined as $k = 6.1\ \mathrm{mol}^{-1}\,\mathrm{l}\,\mathrm{min}^{-1}\,[\mathrm{H}^+]^{-1}$ at 39 °C, in good agreement with the literature. Along the heterogeneous step of the reaction, the ultrasound maintains an additional quantity of water under a virtual state of dissolution besides the water dissolved due to the homogenizing effect of the alcohol produced in the reaction. The forced virtually dissolved water is probably represented by water at the TEOS–water interface during the heterogeneous step of the reaction. The mean radius of the heterogeneity represented by water dispersed in TEOS phase, while hydrolysis has not started yet, was evaluated as about 290 Å. The HCl concentration accordingly increases the hydrolysis rate constant but its fundamental role on the immiscibility gap of the TEOS–water–ethanol system has not been unequivocally established.

PACS: 81.20.Fw; 82.70.Gg
Keywords: Tetraethoxysilane; Sono-hydrolysis; Sol–Gel

1. Introduction

A large variety of glass and glass ceramics has been obtained by sol–gel process from the hydrolysis of tetraethoxysilane (TEOS) [1]. Since the TEOS–water system exhibits an immiscibility gap, a homogenizing medium, as alcohol, is frequently used to promote hydrolysis in the conventional method. Ultrasound is an alternative and efficient method to promote hydrolysis of alkoxides without using alcoholic solvent for homogenization of the mixtures [2]. Due the immiscibility gap, the hydrolysis rate is practically zero at the beginning of the ultrasonic process of mixing. Ultrasound acts as an effective starter for the reaction by fast mixing the system and promoting cavitation which increases the hydrolysis rate, in case of the cavitating bubble to be at the interface of the phases or to migrate from a phase to the other [3]. This effect is equivalent to an increase of the contacting area between alkoxide and water. The product of hydrolysis (alcohol and silanol) helps the mutual dissolution, causing a further enhancement of the reaction rate, until it eventually reaches a maximum value, at a time t_p, and then decreases as a function of the reactant consumption.

In a previous work [4] the hydrolysis rate of the heterogeneous TEOS–water system was measured as a function of the sonication time for several pH values. The thermal peak, which arises due to the heat release of the hydrolysis reaction under ultrasound stimulation, has been measured by a calorimetric method [5] and corrected by the temperature increase effect [4]. So, isothermal hydrolysis rate curves have been obtained and the hydrolysis rate constants were determined at the asymptotic part of the curves, when the system goes to a homogeneous behavior. However, the method is very imprecise due to the critical experimental base line subtraction at the asymptotic part of the curves. Furthermore, it was suggested that the immiscibility gap of

* Corresponding author. Fax: +55-19-526-2237.
E-mail address: vollet@rc.unesp.br (D.R. Vollet).

1350-4177/02/$ - see front matter
PII: S1350-4177(01)00120-1

TEOS–water–ethanol system is diminished as the pH is increased [6]. However, we could not study the immiscibility gap in presence of the acid catalyst since acid starts the hydrolysis and an equilibrium situation could not be attained. Then, in this work, we decided to fit an earlier dissolution and reaction modeling [7] with the hydrolysis rates, which have been determined in the above mentioned previous work [4], to probe the effect of the ultrasound in the hydrolysis pathway and of the pH on the immiscibility gap of TEOS–water–ethanol system.

2. Material and ultrasound procedure

TEOS (Wacker 97%), distilled and deionized (Permution) water, and HCl (Merck 37%) were used to prepare heterogeneous TEOS–water–HCl reactant mixtures of constant volume ($V_T \sim 27$ ml). The initial TEOS and H_2O concentrations were, respectively, $A_0 = 3.38$ M and $B_0 = 13.5$ M ($r = [H_2O]/[TEOS] = 4$), and the HCl concentration was varied to cover the nominal pH range between 0.8 and 2.0. The mixtures were submitted to a constant power (60 W) of ultrasonic radiation by using a Sonics & Material VC600 apparatus, operating at a 20 kHz, with a 13 mm diameter titanium transducer driven by an electrostrictive device. The reaction cell and the temperature control are described elsewhere [4]. The experimental conditions allow us to maintain a heat flow steady state through the medium under high convection, between the ultrasonic heat source and the external environment. Under the condition of heat flow steady state, a steady state temperature (T_R) is held constant at about 5 °C above the external circulating bath temperature (T_e) during an induction time (t_i), whose duration depends mainly on the pH, as experimentally observed in this system [4]. The starting of the hydrolysis yields an additional increase of the medium temperature $\Delta T_t = T - T_R$, where T is the instantaneous mixture temperature, which accounts for the instantaneous hydrolysis rate. The hydrolysis rates were obtained from ΔT_t measurements as a function of the sonication time and the HCl concentration at the condition $T_e = 34.5$ °C [4]. The hydrolysis rates were determined in absolute concentration × time^{-1} units by integration and normalization of the thermal peak ΔT_t. The hydrolysis rates were also converted to isothermal ones at $T = 39$ °C using the activation energy as measured in Ref. [5] and the procedure described in Ref. [4]. The results are shown in Fig. 1.

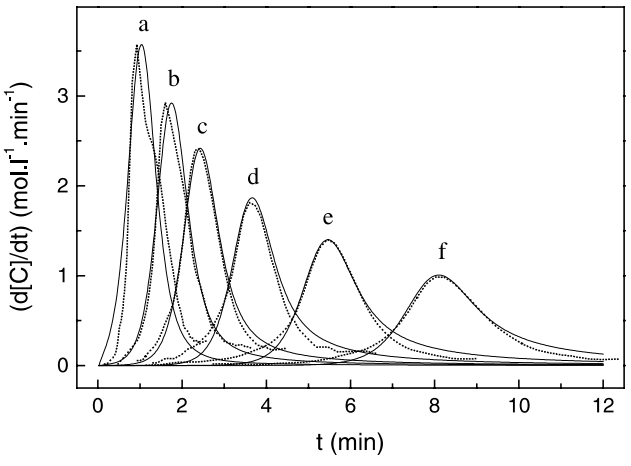

Fig. 1. Theoretical (—) and experimental (···) hydrolysis rates as a function of the sonication time and the HCl concentration. [H^+] raging according to the samples a–f in Table 1.

3. The dissolution and reaction modeling

In the followings we resume the main assumptions of the kinetic model based on the dissolution and reaction mechanism, which has been presented elsewhere [3,7]. The hydrolysis reaction between TEOS (A) and water (B) to yield $Si(OH)_4$ (C) and ethanol (D) can be written as

$$A + B \rightarrow C + D \tag{1}$$

Since A and B are immiscible and the A-phase takes most of the total volume ($\sim 0.76 V_T$ for $r = 4$), we assume, to simplify, a mechanism of dissolution of B in A and subsequent reaction in A-phase, according to the following steps:

$$B \xrightarrow{k_o} B_s \tag{2a}$$

$$B + D_s \xrightarrow{k_d} B_s \tag{2b}$$

$$A + B_s \xrightarrow{k_H} C + D_s \tag{2c}$$

where B_s represents the water dissolved in the A-phase, D_s the ethanol produced in the reaction in the A-phase, k_o and k_d the dissolution rate constants associated to the ultrasound and the alcohol producing dissolution, respectively, and k_H the hydrolysis rate constant. Assuming first order on B for k_o, second order on B and D_s for k_d, and second order on A and B_s for k_H, we obtain the following rate equations for B_s and C production:

$$\frac{d[B_s]}{dt} = (k_o + k_d 4[C])(B_0 - 4[C] - [B_s]) - k_H(A_0 - [C])[B_s] \tag{3}$$

and

$$\frac{d[C]}{dt} = k_H(A_0 - [C])[B_s], \tag{4}$$

where 4 accounts for the stoichiometry of the hydrolysis reaction, A_0 and B_0 are the initial quantities of TEOS and water, respectively, and [ ] denotes the time dependent molar concentration of the species.

4. Results and discussion

4.1. Fitting the reaction and dissolution modeling

Eqs. (3) and (4) were solved using a Runge–Kutta (RK4) subroutine. The apparent best fit with the experimental peak time (t_p), the peak height and the peak half-width was obtained by changing k_o, k_d, and k_H according to the results in Table 1. We decided to fit the parameter $k = k_H[H^+]^{-1}$ instead of k_H, since Ref. [4] suggests that $k_H \propto [H^+]$ because the plot of $\log k_H$ versus $\log[H^+]$ was found to be linear with slope equal to 1. The ionic hydrogen molar concentration, $[H^+]$, was evaluated from the experimental [HCl] preparation. So $k_H[H^+]^{-1}$ should be proportional to the acid specific hydrolysis rate constant and a constant value should be expected for k in the last column of Table 1.

Fig. 1 shows theoretical hydrolysis rates compared to the experimental ones as a function of the sonication time and the HCl concentration. The modeling fits very well with the experimental hydrolysis rates in all cases, except at extremely high acid concentration. We should emphasize that the modeling is just a simplified approximation and it intends to describe only the dissolution and hydrolysis process. So, it is assumed that hydrolysis is resolved from polycondensation [8] but, if some polycondesation is present anyway, it brings no meaningful contribution to the measured thermal peak.

The values for k in Table 1 are all close to a constant value about 6.1 $mol^{-1}\,l\,min^{-1}\,[H^+]^{-1}$. This result is about 25% greater than that obtained earlier (4.6 $mol^{-1}\,l\,min^{-1}\,[H^+]^{-1}$) by using the asymptotic part of the experimental hydrolysis rate curves in determining the hydrolysis rate constants [4]; but, as pointed out, the earlier method is very imprecise due to the critical experimental base line subtraction at the asymptotic part of the curves. Aelion et al. [9] have found $k = 0.051$ $mol^{-1}\,l\,s^{-1}\,[HCl]^{-1}$, or 3.06 $mol^{-1}\,l\,min^{-1}\,[HCl]^{-1}$, at 20 °C for the hydrolysis rate constant of the TEOS using dioxane as a solvent. They have found that this value is not substantially different for other solvents [9]. If we assume an Arrhenius relationship for the rate constant together with the activation energy which they have measured (6.8 kcal/mol) [9], we can transform their value at 20 °C to obtain $k = 6.1$ $mol^{-1}\,l\,min^{-1}\,[HCl]^{-1}$ at 39 °C, in excellent agreement with the result of the present work. Then the hydrolysis rate constants are similar in both methods: solventless ultrasound-stimulated hydrolysis and conventional solvent mediated hydrolysis. So, the main effect of the ultrasound in the solventless hydrolysis reaction is associated to the starting and the homogenization process.

The values of k_d in Table 1 are all close to a constant value around 0.4–0.5 $mol^{-1}\,l\,min^{-1}$. For the highest acid concentration k_d was found to be a lower value (0.23 $mol^{-1}\,l\,min^{-1}$) but the fitting process was found not so good. Therefore, it seems that the variation of pH does not play a fundamental role on the alcohol dissolution rate constant. It may mean that the TEOS–water–alcohol immiscibility gap might not be influenced by the pH variation. It should be noted that k_d is determined under conditions of simultaneous sonication. So, k_d should be interpreted as the ultrasound-stimulated alcohol dissolution rate constant. The magnitude of k_d could change with the ultrasound power.

The values of k_o in Table 1 increase exponentially with the HCl concentration. We interpreted such a variation as the following. According to Eq. (4), the hydrolysis rate, $d[C]/dt$, is practically zero during the induction time (t_i) in which $[B_s] \sim 0$. The induction period depends on the initial alcohol production rate, or simply on the initial hydrolysis rate. Ultrasound forces the starting of the hydrolysis through the Eq. (2a) with the rate constant k_o. We expected the ultrasound to have high efficiency to disperse the phases (promoting cavitation) at the beginning of the process, but the efficiency to dispersion is rapidly lost as the system tends to a dynamic equilibrium. Hence, k_o really behaves as a function of the sonication time, which diminishes with the time. Fig. 2 shows, through the straight line obtained by plotting $\ln k_o$ versus $t_i^{1/2}$, that k_o is well described by an empirical relationship with the induction time t_i given by

$$k_o = 0.54\exp(-5.9t_i^{1/2}), \tag{5}$$

where k_o is expressed in min^{-1} and t_i in min.

Under these conditions, the initial virtually dissolved water at the time t_i, $[B_s]_0$, while no hydrolysis has been occurred yet, could be determined by integration, between $t = 0$ and $t = t_i$ of the rate equation resulting exclusively from the process 2a, using Eq. (5) and

Table 1
Ultrasound and alcohol producing dissolution rate constants and hydrolysis rate constant as determined by fitting the simplified modeling to the experimental hydrolysis rate at 39 °C as a function of the HCl concentration

Sample	$[H^+]$ ($mol\,l^{-1}$)	k_o (min^{-1})	k_d ($mol^{-1}\,l\,min^{-1}$)	k_H ($mol^{-1}\,l\,min^{-1}$)	$k = k_H[H^+]^{-1}$
a	0.143 ± 0.003	$(3.3 \pm 0.2) \times 10^{-2}$	0.23 ± 0.02	0.87 ± 0.05	6.1 ± 0.2
b	0.059 ± 0.001	$(3.5 \pm 0.2) \times 10^{-3}$	0.38 ± 0.03	0.37 ± 0.02	6.2 ± 0.2
c	0.038 ± 0.001	$(6.0 \pm 0.3) \times 10^{-4}$	0.45 ± 0.04	0.23 ± 0.01	6.1 ± 0.2
d	0.0240 ± 0.0006	$(4.0 \pm 0.2) \times 10^{-5}$	0.52 ± 0.05	0.139 ± 0.008	5.8 ± 0.2
e	0.0150 ± 0.0004	$(3.1 \pm 0.1) \times 10^{-6}$	0.50 ± 0.04	0.092 ± 0.005	6.1 ± 0.2
f	0.0098 ± 0.0002	$(3.5 \pm 0.1) \times 10^{-7}$	0.44 ± 0.04	0.060 ± 0.003	6.1 ± 0.2

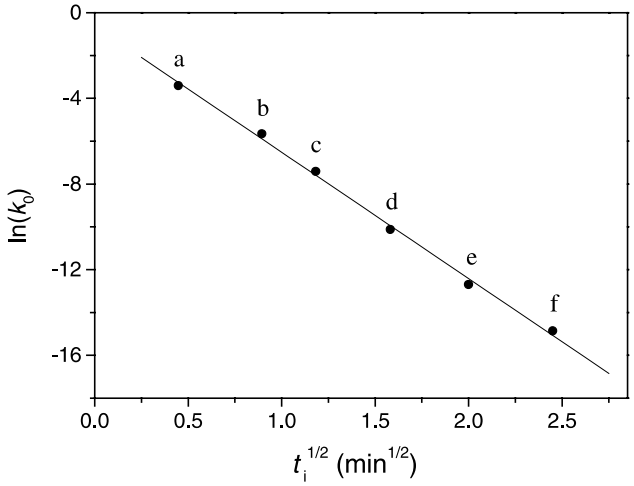

Fig. 2. Plot illustrating the empirical relationship between the ultrasound dissolution rate constant and the induction time given by Eq. (5).

assuming the undissolved water approximately a constant value equal to $B_0 = 13.5$ M. Fig. 3 shows the fraction $[B_s]_0/B_0$ obtained from the mentioned integration as a function of the sonication time. This result shows that the initial fraction of virtually dissolved water reaches rapidly a stationary value about 0.031, or 3.1%, after around 1 min sonication. This stationary value remains constant along the sonication process while hydrolysis has not started, or during the induction time t_i, and it could depend on the ultrasound power. The hydrolysis rate is high enough for high acid concentrations to start the hydrolysis before the mentioned stationary value has been attained.

4.2. The reaction pathway

The initial virtually dissolved water should be represented by water at the contact area between TEOS and water phases. Ultrasound maintains high subdivision of the phases, caused by fast mixing and promotion of cavitation, and enabling the system to have a large contact area between TEOS and water. We thought the importance for hydrolysis of the vapor phase within the cavitating bubble is more meaningful when the mixture becomes homogeneous. Assuming that water is at the interface, we would have $n_{SUP} \sim [B_s]_0 V_T$ moles of water at the interface when the induction period has finished. If each water molecule has a cross-sectional area equaling $S_1 \sim 10$ Å$^2 = 10^{-19}$ m^2, we would have a total interface area equaling $S = n_{SUP} S_1 \sim N_A [B_s]_0 V_T S_1$, where N_A is Avogadro's number. This yields $S \sim 680$ m^2 or about 27 m^2/g. Since the initial volume of the water phase is about $0.24 V_T$ the mean radius of the particulate water dispersed in the system, assuming an equivalent spherical dispersion, would be about $r_{sph} = (3)0.24 V_T / S \sim 2.9 \times 10^{-8}$ m ~ 290 Å.

Fig. 4 shows the time dependence of the apparent dissolved water in the TEOS phase, $[B_s]$, as a function of the acid concentration until the end of the hydrolysis process. After hydrolysis has started, $[B_s]$ is the result of the both dissolution processes 2a and 2b. $[B_s]$ reaches a maximum value at approximately the peak time (t_p), characteristic of each acid concentration. The maximum attained value of $[B_s]$ is higher as the acid concentration diminishes but it tends to a constant value at low acid concentrations. This means that at high acid concentration dissolution is rather the controlling step of the overall process, while at low acid concentration hydrolysis is the controlling step of that. To corroborate this observation, Table 1 shows that $k_d = 0.23$ mol^{-1} l min^{-1} $< k_H = 0.87$ mol^{-1} l min^{-1} for $[H^+] = 0.143$ M and $k_H = 0.060$ mol^{-1} l min^{-1} $< k_d = 0.44$ mol^{-1} l min^{-1} for $[H^+] = 0.0098$ M.

Fig. 5 shows $[B_s]$ as a function of the reacted quantity [C]. For low acid concentrations, $[B_s]$ increases rapidly

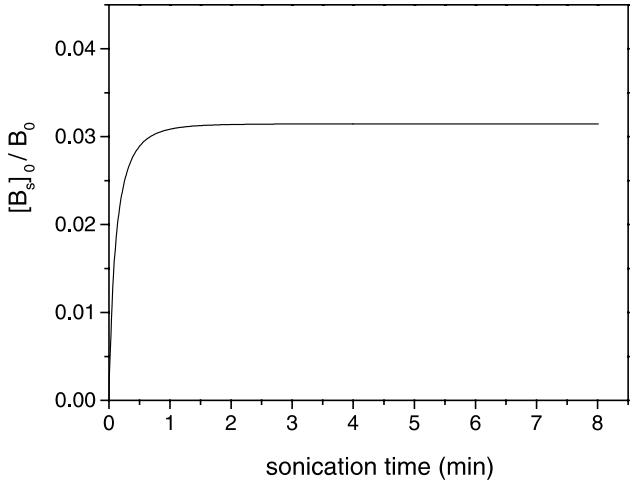

Fig. 3. Fraction of virtually dissolved water in TEOS phase as a function of the sonication time while hydrolysis has not started.

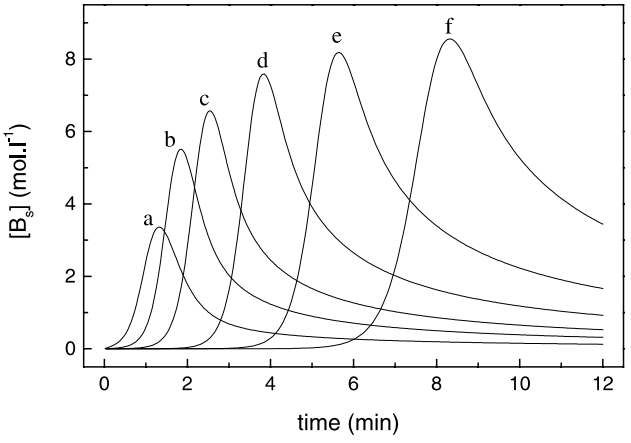

Fig. 4. Time dependence of the apparent dissolved water in the TEOS phase as a function of the acid concentration along the overall dissolution and hydrolysis process.

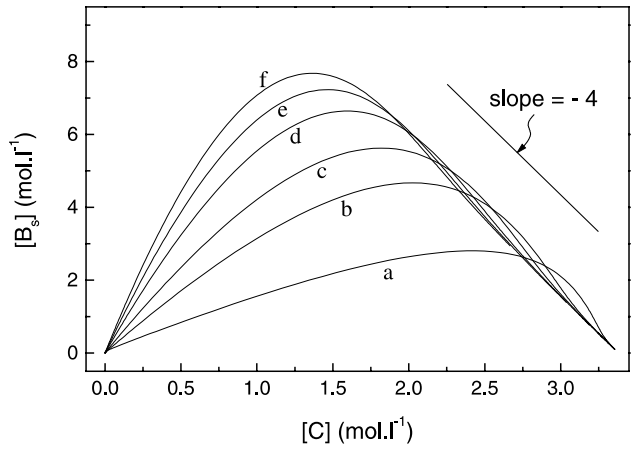

Fig. 5. The apparent dissolved water in the TEOS phase as a function of the reacted quantity.

accompanying [C] at the beginning of the process, while the dissolution and reaction mechanism predominates, it reaches a maximum value at around [C] $\sim$ 1.3–1.8 M and finally decays following approximately a linear relationship given by $[B_s] = B_0 - 4[C]$, as shown by the slope $= -4$ at the final linear part of the curve in Fig. 5. The decay law $[B_s] = B_0 - 4[C]$ should be expected when the remaining water in the system is quite dissolved so hydrolysis goes on as in a homogeneous medium. As the acid concentration increases the homogeneous behavior law becomes less apparent and it definitively does not apply at all to $[H^+] = 0.143$ M.

The reaction pathway can more familiarly be visualized in a ternary diagram representing the molar fraction of the reactants (TEOS and H_2O) and the product of the hydrolysis (CH_2CH_3OH and $Si(OH)_4$), as shown in Fig. 6. We included ethanol and $Si(OH)_4$ as product

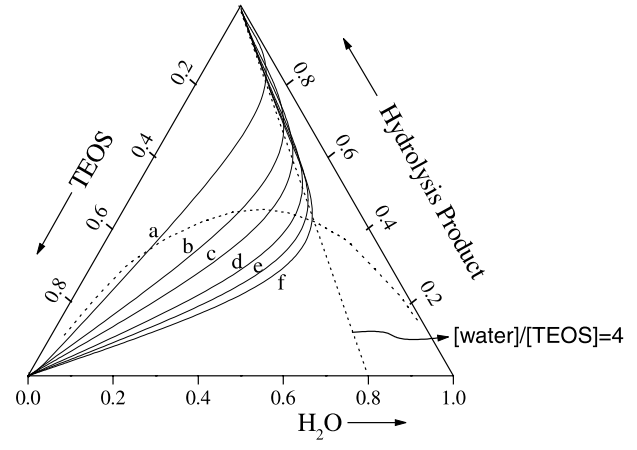

Fig. 6. Ternary diagram of the molar fraction of TEOS, water and product of the hydrolysis (ethanol + $Si(OH)_4$) showing the reaction pathway under ultrasound stimulation as a function of the HCl concentration. The dashed curve represents the immiscibility gap of the TEOS–water–ethanol system drawn from the Kamiya and Yoko data [6].

to allow a ternary representation. We should bear in mind that product represents 4 mol of ethanol and 1 mol of $Si(OH)_4$, so its molar fraction in the diagram of Fig. 6 is composed by 80% ethanol and 20% $Si(OH)_4$. To convert the molar concentration of the specie i in the TEOS phase, C_i, to its corresponding molar fraction, X_i, we have employed the relationship $X_i = (V/n)C_i$, where V is the instantaneous volume of the TEOS phase and n the instantaneous total number of moles in the TEOS phase. (V/n) and X_i were evaluated as a function of the reaction evolution from the initial conditions and from [C] and $[B_s]$ data. The curves in Fig. 6 denote the molar fraction of the water, X_{BS}, which is virtually dissolved in the TEOS phase along the hydrolysis reaction pathway. The immiscibility gap of the non-acidulated TEOS–water–ethanol system was drawn as the dashed curve in Fig. 6 from the Kamiya and Yoko data [6].

The experimental X_{BS} was found to be even greater than the water solubility in presence of ethanol, except for extremely high acid concentration. We are tempted to attribute this result to the acid improving dissolution effect causing diminution of the immiscibility gap, as pointed out by Kamiya and Yoko [6]. However, the effect of the acid improving dissolution was found changing on the contrary of the acid concentration increase. So, we attribute the excess X_{BS} to the additional virtually dissolved water in TEOS phase caused by continuous ultrasonication after the starting of the hydrolysis. Such additional virtually dissolved water should also be represented by water at the contact area between TEOS and water phases, except by the higher subdivision state of the phases, now allowed by the presence of the ethanol produced in the reaction. We do not believe that ultrasound could be able to really solve any additional water. X_{BS} increases with the advance of the reaction until all remaining water in the system had been dissolved. At this point, the system crosses the immiscibility gap becoming homogeneous, so hydrolysis follows the homogeneous pathway along the linear dashed line defined by [water]/[TEOS] = 4 in the diagram of Fig. 6. Such a pathway is fairly well followed by the system under low acid concentration, while hydrolysis is the controlling step during the heterogeneous step of the process. For high acid concentration ($[H^+] = 0.143$ M) the reaction pathway along the heterogeneous step of the process follows approximately the solubility line (the dashed curve in Fig. 6) at the side of the TEOS phase. This result is expected since the dissolution was found to be the controlling step for high acid concentration.

The calculated homogeneous part of the pathway showed in Fig. 6, which goes from the crossing point of the immiscibility gap until the intercept with the straight dashed line defining [water]/[TEOS] = 4, represents an unreal trajectory that the simplified modeling could not be able to prevent. Indeed, there is a discontinuity in the pathway when the system crosses the immisciblity gap to

follow the homogeneous trajectory [water]/[TEOS] = 4. The hydrolysis rate can be cast as $d[C]/dt = k_H[A][B_s]$. The modeling finds out an equivalent trajectory to give the same medium value for the product $[A][B_s]$ which would be observed along the real trajectory [water]/[TEOS] = 4.

5. Conclusions

The simplified dissolution and reaction modeling employed in this study to probe the hydrolysis of TEOS in heterogeneous TEOS–water–HCl mixtures fits very well with the experimental hydrolysis rates measured as a function of the sonication time, for the nominal pH ranging from 0.8 to 2.0. The acid specific hydrolysis rate constant was determined as $k = 6.1\ \mathrm{mol}^{-1}\,\mathrm{l}\,\mathrm{min}^{-1}\,[H^+]^{-1}$ at 39 °C, in good agreement with the literature.

During the induction time in which the hydrolysis has not started, the initial fraction of virtually dissolved water in TEOS phase by the ultrasound action reaches rapidly a stationary value. The mean radius of the heterogeneity represented by water dispersed in TEOS phase at this stage was evaluated as about 290 Å.

Along the heterogeneous step of the hydrolysis reaction, an additional quantity of water is maintained under a virtual state of dissolution, forced by the ultrasound action, besides that water dissolved due to the homogenizing effect of the alcohol produced in the reaction. When the system crosses the immisciblity gap of the TEOS–water–ethanol ternary diagram the hydrolysis pathway change rapidly to the homogeneous trajectory defined by the relation [water]/[TEOS] = 4.

The HCl concentration accordingly increases the hydrolysis rate constant, but its fundamental role on the immiscibility gap of the TEOS–water–ethanol system has not unequivocally been established.

References

[1] C.J. Brinker, G.W. Scherer, in: Sol–Gel Science: The Physics and Chemistry of Sol–Gel Processing, Academic Press, San Diego, 1990, p. 108.
[2] M. Tarasevich, Am. Ceram. Bull. 63 (1984) 500.
[3] D.A. Donatti, D.R. Vollet, A. Ibañez Ruiz, J. Sol–Gel Sci. Technol. 18 (2000) 5.
[4] D.A. Donatti, D.R. Vollet, J. Non-Cryst. Solids 208 (1996) 99.
[5] D.A. Donatti, D.R. Vollet, J. Sol–Gel Sci. Technol. 4 (1995) 99.
[6] K. Kamiya, T. Yoko, J. Mater. Sci. 21 (1986) 842.
[7] D.R. Vollet, D.A. Donatti, J.R. Campanha, J. Sol–Gel Sci. Technol. 6 (1996) 57.
[8] J.C. Pouxviel, J.P. Boilet, J.C. Beloeil, J.Y. Lallemand, J. Non-Cryst. Solids 89 (1987) 345.
[9] R. Aelion, A. Loebel, F. Eirich, J. Am. Chem. Soc. 72 (12) (1950) 5705.